View metadata, citation and similar papers at core.ac.uk
brought to you by CORE
provided by KnowledgeBank at OSU

10.1149/1.2789221, copyright The Electrochemical Society

Corrosion Inhibition of AA2024-T3 by Vanadates

M. Iannuzzi and G. S. Frankel
Fontana Corrosion Center
The Ohio State University
Columbus, OH 43210

The speciation of vanadate solutions and the resulting inhibition of oxygen reduction and corrosion of AA2024-T3 were investigated. ^{51}V NMR is very useful for assessing vanadate speciation. Clear metavanadate solutions contain no decavanadate, which forms whenever the pH was decreased by the addition of acid. Orange decavanadate solutions contain no monovanadate, even when the pH is adjusted to high values. Monovanadate is a potent inhibitor in contrast to decavanadate. Inhibition by monovanadate seems to result from an adsorption mechanism rather than reduction. Monovanadate effectively protects S phase particles. Aging of high-pH decavanadate solutions does not improve the inhibition performance or result in complete depolymerization of the decavanadate.

Introduction

Vanadium-based oxyanions, also referred to as vanadates, have been previously investigated as corrosion inhibitors for Al alloys [1-4]. However, they have not gained much attention in part due to the relatively large solubility of vanadium oxides in aqueous solutions and their complicated coordination chemistry (1-4). Vanadates exhibit several protonation/deprotonation reactions, as well as polymerization to form oligomers of varied molecular weight, depending upon pH and concentration (5-9). In general, all the polymerized species are referred to as isopolyanions or isopolymetallates (7, 9-11). According to ^{51}V and ^{17}O NMR spectroscopy, the observed oligomers in the range of pH 7-9 and at varied vanadate concentrations are the monovanadates (V_1), divanadates (V_2), cyclic tetravanadates (V_4) and cyclic pentavanadates (V_5) (12-14). These oligomers (V1-V5) are referred to as metavanadates. In contrast, decavanadates are stable in the pH range from 2 to 6 but can form in solutions of higher pH due to local acidification of the solution (5, 9, 13, 15, 16). Polymerization to V_{10} is rapid and the mechanism of formation is not well understood. De-polymerization of V_{10}, on the other hand, is very slow (15). A speciation diagram is shown in Figure 1 for reference (9).

The main objective of this work is to characterize the vanadate system relevant to Al corrosion and address the mechanisms of corrosion protection of AA2024-T3 by solutions containing different vanadate oligomers.

Experimental

Materials and sample preparation: Commercially available sodium vanadium oxide, 98% $NaVO_3$, and reagent-grade sodium chloride from Sigma-Aldrich were used. All solutions were prepared with 18.2 MΩ-cm deionized water. Unless otherwise noted,

Downloaded 29 Jun 2011 to 128.146.58.90. Redistribution subject to ECS license or copyright; see http://www.ecsdl.org/terms_use.jsp

metavanadate solutions were prepared by dissolving $NaVO_3$ in 0.5 M NaCl and adjusting the as-prepared pH to the higher value of 8.71. Orange solutions containing decavanadates were prepared by acidification of the clear solutions to pH 4, and subsequent re-adjustment to pH 8.71. For simplicity, these solutions will be referred to as orange decavanadate and clear metavanadate solutions, respectively.

Samples were cut from two different AA2024-T3 panels (nominal composition 3.8-4.9 % Cu, 1.2-1.8 % Mg, 0.3-0.9 % Mn, 0.5 % Fe, 0.5 % Si, 0.25 % Zn, 0.1% Cr, 0.05 % Ti, balance Al) that were 1 and 5 mm thick, respectively. The samples were mounted in epoxy resin; ground through 1200 grit SiC papers (Buehler), and polished with 3 and 1 μm diamond paste (Buehler). Ethyl alcohol (< 0.2% water) was used as a lubricant during all the surface preparation stages to minimize corrosion damage during grinding and polishing.

Nuclear Magnetic Resonance Spectroscopy (NMR): Procedures for ^{51}V NMR described in the literature were followed (12-15, 17-19). High resolution ^{51}V (105.2 MHz) spectra were obtained at room temperature utilizing a Bruker DPX 400 MHz superconducting magnet. Other experimental details have been reported elsewhere (20).

Chronoamperometry: The effects of metavanadate and decavanadate injections at varied applied potentials were investigated by measuring the time evolution of the cathodic current at constant applied potential. Concentrated solutions containing metavanadates or decavanadates were injected to make 5 mM total vanadate after mixing. The final pH after mixing was 7.6 in all the experiments. A VoltaLab PGP-201 potentiostat was used with a platinum mesh counter-electrode and a SCE reference electrode.

X-ray photoelectron spectroscopy: Vanadium at the surface was investigated by XPS. Cu and AA2024-T3 samples were polarized at fixed cathodic potentials for 3 h. Concentrated 150 mM metavanadate and decavanadate solutions were injected after 15 min to make 5 mM total vanadate after dilution. XPS spectra were acquired using a Kratos Axis Ultra with a monochromated Al x-ray source at 130 W.

Results and Discussion

Minimum pH for V_{10} Formation

As-prepared, $NaVO_3$ solutions remain colorless with a pH that linearly increases with total vanadium concentration (20). Acidification with concentrated HCl to adjust bulk pH produces a change in color to orange indicating the formation of decavanadates. The determination of the minimum pH that causes V_{10} formation was investigated. Aliquots of colorless 150 mM $NaVO_3$ + 0.5 M NaCl solutions were added to beakers containing 0.5 M NaCl solutions with initial pH (pH_0) varying from 1 to 12. The final pH after mixing, pH_f, was monitored and determined as a function of pH_0 (20). Figure 2 shows the pH_f as a function of pH_0. The color change associated with V_{10} formation was only triggered if $pH_0 \leq 3$, independent of final vanadate concentration. Interestingly, for 100 mM and 50 mM final vanadate concentrations, pH_f was equal to 8.4 independent of pH_0 for $3<pH_0<12$. For 5 mM total vanadate, pH_f was equal to 7.6 independent of pH_0 for $4<pH_0<12$. In other words, to create vanadate solutions of concentration 5 mM or higher

Downloaded 29 Jun 2011 to 128.146.58.90. Redistribution subject to ECS license or copyright; see http://www.ecsdl.org/terms_use.jsp

with pH less than 7.5, the vanadates must be mixed with solutions having pH less than 3-4. A direct implication of these findings is the practical impossibility of adjusting the pH of clear $NaVO_3$ solutions without producing a change in color and speciation.

Nuclear Magnetic Resonance Spectroscopy

In part as a consequence of the role played by vanadates in modifying several biochemical processes, vanadate speciation has been the subject of several review studies that characterized the system in detail (12-21). Modern high-field NMR gives high quality structural data and quantitative information regarding speciation and concentration of a large variety of compounds in aqueous and non-aqueous solvents (22). The only limitation of NMR is the inability of detecting minor components with overlapping or coincident chemical shifts (20, 22).

Typical ^{51}V NMR spectra for a 100 mM decavanadate solution and a 100 mM metavanadate solution both adjusted to pH 8.71 are shown in figures 3a and b (20). The peaks are labeled based on assignments reported in the literature (5-7, 12-20). NMR peaks are proportional to the species concentration (22). Summations of the peak areas of spectra such as those in figures 3a and 3b from both decavanadate and metavanadate solutions of varying concentration are given in figures 3c and d, respectively. In both cases, the sum of *n* times the area under the peaks, where n = 1, 2, 4, 5 or 10, linearly scaled with total vanadium concentration, thereby proving the validity of the peak assignment and providing a calibration of the method.

Figure 4 shows changes in speciation associated with pH adjustment (20). A typical ^{51}V NMR spectrum of a 100 mM clear metavanadate solution at pH 8.71 is shown in figure 4a. The oligomers present in such conditions are the monovanadate (V_1), the divanadate (V_2), the tetravanadate (V_4) and the pentavanadate (V_5) as has been reported previously (5-7, 12, 14, 16, 20, 22). At low concentrations (1 to 5 mM $NaVO_3$) V_1 is the predominant species, whereas at higher concentrations, such as the case of Figure 4a, the oligomers of higher molecular weight become predominant (12, 13). When the clear metavanadate solutions are acidified to pH 4, all the metavanadates polymerize to form an orange decavanadate solution exclusively containing V_{10} oligomers, within the detection limit of the instrument (Figure 4b). Increasing the pH of the decavanadate solution produces the partial de-polymerization of V_{10} to give V_5, V_4, and V_2 (Figure 4c). At low concentrations (1 to 5 mM $NaVO_3$), V_{10} is the predominant species and V_2 is the main metavanadate in these solutions with pH adjusted back to high values. As [$NaVO_3$] increases, V_4 becomes the predominant metavanadate, as in the case of Figure 4c.

Effects of Vanadates on the Anodic Dissolution Kinetics

The corrosion inhibiting effects of orange solutions containing decavanadate but no monovanadate and clear solutions containing metavanadates (V_1 through V_5) but no decavanadate were determined at the fixed pH of 8.71. Anodic polarization curves of AA2024-T3 in deaerated 0.5 M NaCl with no inhibitor are characterized by two breakdown potentials if the sample is polished in the absence of water to minimize S-phase attack (23). The current increases after the first breakdown potential, reaches a maximum, decreases to an intermediate minimum value and then increases again after the second breakdown potential, figure 5 (33). The first breakdown (at E_{P1}) is related to the

Downloaded 29 Jun 2011 to 128.146.58.90. Redistribution subject to ECS license or copyright; see http://www.ecsdl.org/terms_use.jsp

transient dissolution of S-phase particles and the second one (at E_{P2}) to matrix and intergranular attack (23). Anodic polarization curves of AA2024-T3 were affected by the presence of 5 mM metavanadate. As observed in figure 5a, the first breakdown potential was not present when metavanadate was added. The pitting potential was similar to E_{P2} in the absence of metavanadates. Since E_{P1} is related to dissolution of Al_2CuMg, the absence of such a transient event seems to indicate that the clear metavanadate solutions suppressed the dissolution of S-phases at least until the potential reached E_{P2}.

E_{P1} also was absent in anodic polarization curves of AA2024-T3 in electrolytes containing decavanadates, Figure 5b. The open circuit potential in the presence of decavanadate was higher than the OCP in 0.5 M NaCl with no inhibitor in deaerated conditions. Anodic polarization curves at varied decavanadate concentrations revealed that at least 5 mM total vanadate is required to protect S-phase dissolution. As in the case of monovanadates, decavanadates might inhibit pit initiation by controlling the initiation of the attack of S-phase particles. However, even though decavanadates reduced anodic dissolution of S-phases, the small reduction of the ORR resulted in a severe attack on the anode surface during split cell experiments.

Effects of Vanadates on the Cathodic Kinetics

Cathodic polarization curves were measured on AA2024-T3 in orange decavanadate and clear metavanadate solutions containing 0.5 M NaCl and varying amounts of $NaVO_3$ (20). Figure 6a compares typical cathodic polarization curves for 100 mM $NaVO_3$ solutions. A cathodic polarization curve in 0.5 M NaCl with no vanadates is also shown for reference. In the absence of inhibitor, the oxygen reduction reaction (ORR) exhibits a limiting current density at a relatively high value reflecting the strong agitation of the electrolyte by a stir bar. Figure 6a shows that orange decavanadate solutions did not reduce the kinetics of ORR significantly. The effects of $NaVO_3$ concentration are summarized in figure 6b. Comparison of the effects of vanadate on ORR kinetics is complicated by the different shapes of the polarization curves, especially at low potentials. The current density values plotted in figure 6b were obtained by extrapolating the linear regions of the cathodic curves to the high potential of -800 mV SCE. Higher vanadate concentrations resulted in larger cathodic currents for the orange decavanadate solutions, supporting the concept that decavanadates are poor inhibitors of the ORR. The small amount of inhibition observed in decavanadate solutions is possibly a consequence of the presence of metavanadates such as V_2 (20).

In contrast to the orange decavanadate solutions, a significant decrease in the rate of oxygen reduction was observed in clear metavanadate solutions. The kinetics of oxygen reduction were reduced by almost four orders of magnitude and no diffusion limiting region was observed, figure 6a. In addition, the threshold for hydrogen evolution was shifted toward more negative overpotentials. In further contrast to the orange decavanadate solutions, inhibition performance increased with increasing vanadate concentration, figure 6b. Since the orange decavanadate solutions contain no V_1 and the clear metavanadate solutions contain no V_{10}, these results suggest that decavanadates are detrimental or ineffective inhibitors and monovanadates provide the best inhibition (20). In this regard, the extent of inhibition imparted by monovanadates is similar to that reported for chromates and dichromates in aqueous solutions (24-26).

Downloaded 29 Jun 2011 to 128.146.58.90. Redistribution subject to ECS license or copyright; see http://www.ecsdl.org/terms_use.jsp

Chronoamperometry

To evaluate the mechanisms of corrosion inhibition by vanadates, experiments at different fixed potentials were performed on Cu and AA2024-T3. The evolution of the current and the effects of injecting either clear metavanadate or orange decavanadate solutions, to make 5 mM total vanadate after mixing, were investigated. Figure 7a shows the effects of clear metavanadate injections for a Cu sample polarized at -600 mV SCE (33). Injection of solution containing monovanadates produced a rapid reduction in cathodic current, with no current peak. The percentage of current reduction, which can also be thought as the inhibition efficiency, reached a maximum value of 76 %. The absence of a current transient suggested a mechanism that did not involve electrochemical reduction.

Results of injecting orange decavanadate solutions on Cu at -600 mV SCE are shown in figure 7b. In contrast to clear metavanadate, injection of the solution containing decavanadates was followed by a sharp increase in negative current. After 60 min, the current was lower than before injection, but only by 27 %. The current peak is associated with the electrochemical reduction of decavanadates. Likewise, according to figure 7b, the reduction of decavanadate is not self-limiting.

Chronoamperometry in deaerated conditions was performed to deconvolute the influence of oxygen. Figure 7c summarizes the effects of injecting 0.5 M NaCl with no inhibitor or 0.5 M NaCl containing clear metavanadate solution into the deaerated 0.5 M NaCl electrolyte at an applied potential of -600 mV SCE for a Cu electrode. Injection of the aerated 0.5 M NaCl solution into the deaerated electrolyte produced a small increase in cathodic current. The current returned to the steady state values within minutes due to the constant purging of the system with Ar. Injection of clear metavanadate solution at 15 min produced a current peak that reached -17 $\mu A/cm^2$. The current peak observed in deaerated conditions might represent the reduction of monovanadates. The reduction of monovanadates was not self limiting and reached a steady state value of about -2.4 $\mu A/cm^2$.

X-ray photoelectron spectroscopy

The objective of this analysis was to detect the presence of vanadium at the surface and, possibly, its oxidation state. Spectra for C, Cu or Al, O and V were recorded. Figure 8 summarizes the oxygen 1s and vanadium 2p spectra for both Cu and AA2024 samples in different conditions (33). The vanadium peaks were at a binding energy in the range of 516.14 to 516.3 eV with an experimental error of 0.2 eV. According to the literature, this binding energy corresponds to a 4+ oxidation state (27). However, the binding energy of V_2O_5 standards also reflected binding energies of V^{4+} species. This suggests that photoreduction of vanadates during XPS analysis likely occurred.

Adsorption Isotherm

The absence of a current transient upon injection of clear metavanadate solutions suggested an inhibition mechanism not involving electrochemical reduction. To evaluate if there was a dependency between inhibition and concentration of metavanadates, adsorption isotherms were constructed using the cathodic polarization plots (33). The

Downloaded 29 Jun 2011 to 128.146.58.90. Redistribution subject to ECS license or copyright; see http://www.ecsdl.org/terms_use.jsp

concentration of clear metavanadates varied from 0.001-5 mM. The extent of inhibition, θ, was determined from $\theta = (i_{(free)} - i_{(inhibitor)})/i_{(free)}$. The values of $i_{(inhibitor)}$ and $i_{(free)}$ were determined by extrapolating the linear regions observed in cathodic polarization plots to the high potential of -700 mV SCE.

Langmuir isotherms gave the best fit of the data, suggesting that there were no lateral interactions between adsorbed molecules, Figure 9. C_i/θ scaled with both monovanadate and total metavanadate concentrations. However, the best fit of the data was obtained using the concentration of monovanadate. The slope was almost unity. Using the data obtained by fitting of the adsorption isotherm, a value of -25.12 kJ/ mol is obtained for the free energy of absorption, ΔG^0_{abs}. This value is in good agreement with data reported in the literature and the negative sign represents that adsorption is spontaneous (28-33). This also suggests that adsorption occurs immediately after injection of the clear metavanadate solution. ΔG^0_{abs} ranging from -15 to -30 kJ/ mol indicates that the molecules are physically adsorbed rather than chemisorbed. Chemisorption is characterized by free energies of about -100 kJ/ mol (9).

Long Term Exposure

A comparison of the long term performance of orange decavanadate and clear metavanadate solutions was carried out by analyzing polarization resistance values, R_P, extracted by the linear polarization technique and by optical inspection after OCP exposure (20). Typical results are shown in figure 10. In the absence of inhibitor, R_P varied between 5 and 10 kΩ-cm^2, and samples were severely pitted after the 24 h experiment. An orange decavanadate solution containing 6.26 mM V_{10} (present in a solution that was initially 100 mM $NaVO_3$) exhibited R_P values that fluctuated between 50 and 300 kΩ-cm^2 initially. However, after about 5 h, R_P decreased with time to 10-30 kΩ-cm^2. In contrast, in a clear metavanadate solution containing 1 mM V_1, significantly higher R_P values were observed. Polarization resistance typically varied between 300-1100 kΩ-cm^2 and was virtually independent of $NaVO_3$ concentration above 1 mM. The low corrosion rate was sustained during the 24 h of exposure. Samples exposed at OCP to orange decavanadate solutions containing NaCl rapidly developed pits that could be observed easily with the unaided eye. In contrast, only small pits were observed after exposure to clear metavanadate + chloride solutions (20).

Aging of Decavanadate Solutions

Since high pH orange decavanadate solutions are not at thermodynamic equilibrium, it was of interest to analyze the effects of solution aging on corrosion inhibition performance. A 100 mM orange decavanadate solution adjusted to pH 8.71 was aged for 10 days (20). Samples were extracted for ^{51}V NMR analysis and electrochemical characterization after 1, 3 and 10 days. The ^{51}V NMR spectrum shows that after 24 h aging the amount of V_{10} was reduced and V_4 became predominant (Figure 11a). However, decavanadate was still present and monovanadate did not form during aging, indicating that the de-polymerization to form V_1 is not favored under these conditions. This suggests that the rate of de-polymerization is extremely slow.

Downloaded 29 Jun 2011 to 128.146.58.90. Redistribution subject to ECS license or copyright; see http://www.ecsdl.org/terms_use.jsp

Cathodic polarization curves did not show significant variations with aging time of the orange decavanadate solutions (Figure 11b). A large limiting current associated with a relatively fast rate of ORR was observed.

Effects of pH on Speciation and Inhibition by Clear Metavanadate Solutions

The effects of pH on speciation of 10 mM clear metavanadate solutions were investigated by ^{51}V NMR (20). Figure 12a summarizes the variation of the concentration of the different oligomers as a function of pH. As pH increased, V_1 rapidly became predominant and V_5 and V_4 peaks diminished. Above pH 9 only signal from V_1 and V_2 was obtained.

Finally, the influence of V_1 concentration, protonation state and pH on inhibition was also addressed (20). Cathodic polarization experiments in 0.5 M NaCl + 10 mM $NaVO_3$ with different pH were carried out and compared with solutions containing no inhibitor at the same pH. All polarization curves in the metavanadate-containing solutions exhibited much lower ORR rates, and there was no clear influence of pH (and thus V_1 concentration) (figure 12b). This suggests that, above a critical concentration, most of the local cathodes at the AA2024-T3 surface are blocked by V_1 (or a combination of V_1 and V_2), which greatly reduces the rate of oxygen reduction (20).

Conclusions

Speciation of vanadate solutions with varying concentrations and pH was studied by ^{51}V NMR. In addition, the mechanisms of corrosion inhibition by vanadates were investigated. The following conclusions can be obtained:

1. Vanadate monomers are not present in solutions containing decavanadates.
2. The presence of V_1 species is critical for corrosion protection.
3. V_1 is a potent inhibitor of O_2 reduction.
4. Decavanadates are not good inhibitors of corrosion and O_2 reduction.
5. Control of O_2 reduction kinetics by V_1 seems to result from an adsorption mechanism.
6. Decavanadates reduce at the surface after injection under potential control.
7. Aging of high pH V_{10} solutions did not improve inhibition performance.
8. $[V_1]$ increases with pH but has no extra beneficial effect on oxygen reduction rate.
9. V_1 protects S phase particles.

References

1. R. G. Buchheit, *ECS PV2002-13, Pennington, NJ* 430 (2002).
2. H. Guan and R. G. Buchheit, *Corrosion* **60,** 284 (2004).
3. M. Kendig and R. G. Buchheit, *Corrosion* **59,** 379 (2003).
4. M. Trypuc and G. Lyjak, *Polish J. App. Chem.* **XLI,** 187 (1997).
5. D. C. Crans and A. S. Tracey, *ACS Symposium Series* **711,** 2 (1998).
6. L. Petterson and K. Elvigson, *ACS Symposium Series* **711,** 30 (1998).
7. L. Petersson, *Molecular Eng.* **3,** 29 (1993).
8. J. J. Cruywagen, *Adv. Inorg. Chem.* **49,** 127 (2000).
9. A. F. Holleman and E. Wiberg, Inorganic Chemistry, Academic Press, Berlin-New York (2001).

Downloaded 29 Jun 2011 to 128.146.58.90. Redistribution subject to ECS license or copyright; see http://www.ecsdl.org/terms_use.jsp

10. L. Bouhedja, N. Steunou, J. Maquet and J. Livage, *J. Solid State Chem.* **162,** 315 (2001).
11. J. Livage, *Chem. Mater* **3,** 578 (1991).
12. E. Heath and O. W. Howarth, *J. Chem. Soc., Dalton Trans.* 1105 (1981).
13. J. W. Larson, *J. Chem. Eng. Data* **40,** 1276 (1995).
14. A. S. Tracey, J. S. Jaswal and S. J. Angus-Dunne, *Inorg. Chem.* **34,** 5680 (1995).
15. M. Aureliano and R. M. C. Gandara, *J. Inorg. Biochem.* **99,** 979 (2005).
16. O. W. Howarth and R. E. Richards, *J. Chem. Soc.* 864 (1965).
17. A. S. Tracey, *Coordination Chemistry Reviews* **237,** 113 (2003).
18. A. S. Tracey, M. J. Gresser and K. M. Parkinson, *Inorg. Chem.* **26,** 629 (1987).
19. A. S. Tracey and C. H. Leon-Lai, *Inorg. Chem.* **30,** 3200 (1991).
20. M. Iannuzzi, T. Young and G. S. Frankel, *J. Electrochem. Soc.* **153,** B533 (2006).
21. D. Rehder, *Coord. Chem. Rev.* **182,** 297 (1999).
22. J. B. Lambert and E. P. Mazzola, Nuclear Magnetic Resonance Spectroscopy: An Introduction to Principles, Applications, and Experimental Methods, Pearson Prentice Hall, Ch 1, New Jersey (1999).
23. W. Zhang and G. S. Frankel, *Electrochim. Acta* **48,** 1193 (2003).
24. W. J. Clark, J. D. Ramsey, R. L. McCreery and G. S. Frankel, *J. Electrochem. Soc.* **149,** B179 (2002).
25. J. Zhao, L. Xia, A. Sehgal, et al., *Surf. and Coat. Tech.* **140,** 51 (2001).
26. M. Kendig, S. Jeanjaquet, R. Addison and J. Waldrop, *Surf and Coat Tech* **140,** 58 (2001).
27. J. Kasperkiewicz, J. A. Kovacich and D. Lichtman, *J. Electron. Spectrosc. Relat. Phenom.* **32,** 128 (1983).
28. P. Kern and D. Landolt, *J. Electrochem. Soc.* **148,** B228 (2001).
29. R. Gasparac, C. R. Martin and E. Stunpnisek-Lisac, *J. Electrochem. Soc.* **147,** (2000).
30. R. G. Nuzzo, R. R. Zegarsky and L. H. Dubois, *J. Am. Chem. Soc.* **109,** 733 (1987).
31. M. Kaminski and Z. Szklarska-Smialowska, *Corr. Sci.* **13,** 553 (1973).
32. W. W. Damaskin, O. A. Pietrij and W. W. Batrakow, Adsorption of Organic Compounds on Electrodes, Plenum Press, p. New York (1971).
33. M. Iannuzzi and G. S. Frankel, accepted for publication in *Corr. Sci.* (2006).

Downloaded 29 Jun 2011 to 128.146.58.90. Redistribution subject to ECS license or copyright; see http://www.ecsdl.org/terms_use.jsp

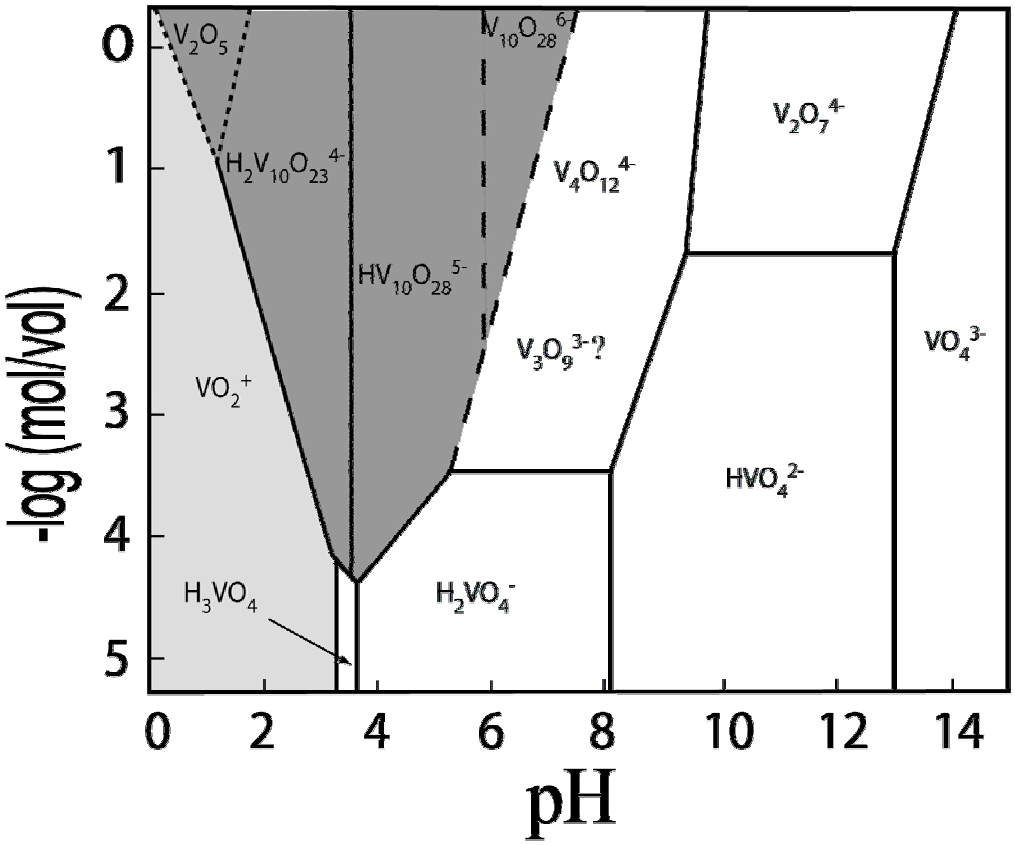

Figure 1. Speciation diagram of vanadates in aqueous solutions (9).

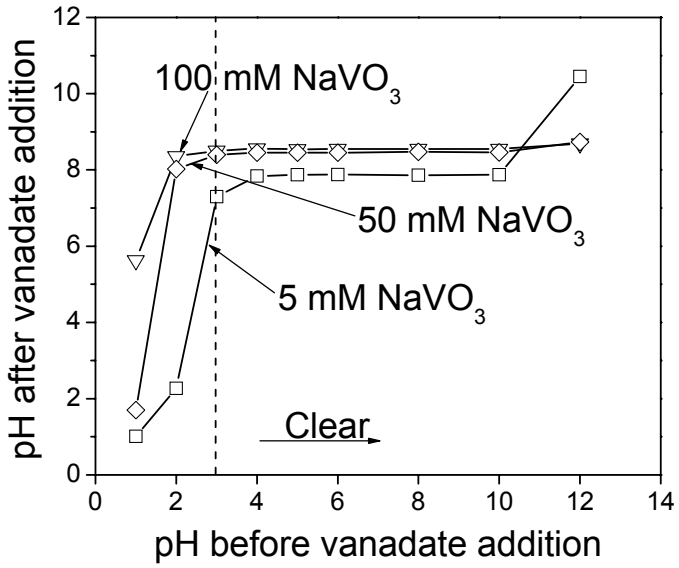

Figure 2. Final pH of solutions formed by mixing metavanadate with solutions of varying initial pH. The concentration refers to the final vanadate concentration after mixing (20).

Downloaded 29 Jun 2011 to 128.146.58.90. Redistribution subject to ECS license or copyright; see http://www.ecsdl.org/terms_use.jsp

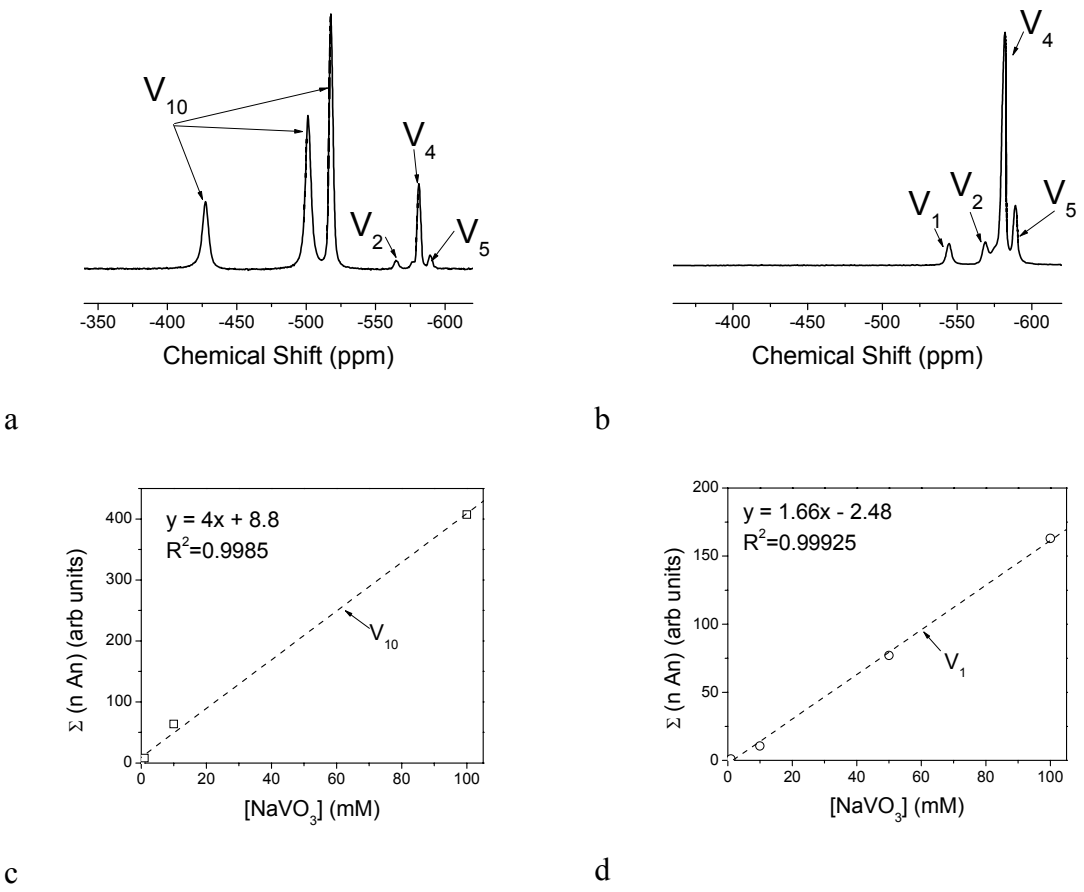

Figure 3. Assignment of ^{51}V NMR peaks and calibration. A) Typical ^{51}V NMR spectrum for an orange decavanadate solution b) typical ^{51}V NMR spectrum for a clear metavanadate solution c) calibration curve for orange decavanadate solutions d) calibration curve for clear metavanadate solutions (20).

Downloaded 29 Jun 2011 to 128.146.58.90. Redistribution subject to ECS license or copyright; see http://www.ecsdl.org/terms_use.jsp

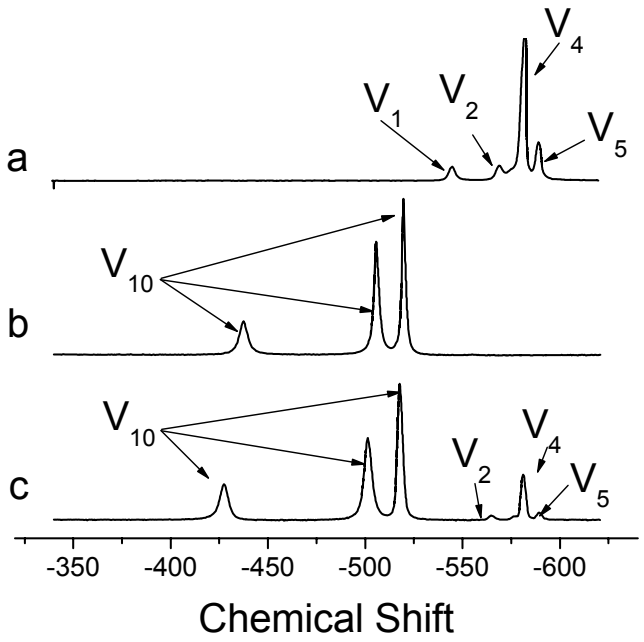

Figure 4. ^{51}V NMR spectra of 100 mM vanadate solution in different conditions: a) as-dissolved pH 8.71, b) acidified to pH 4, c) acidified and re-adjusted to pH 8.71 (20).

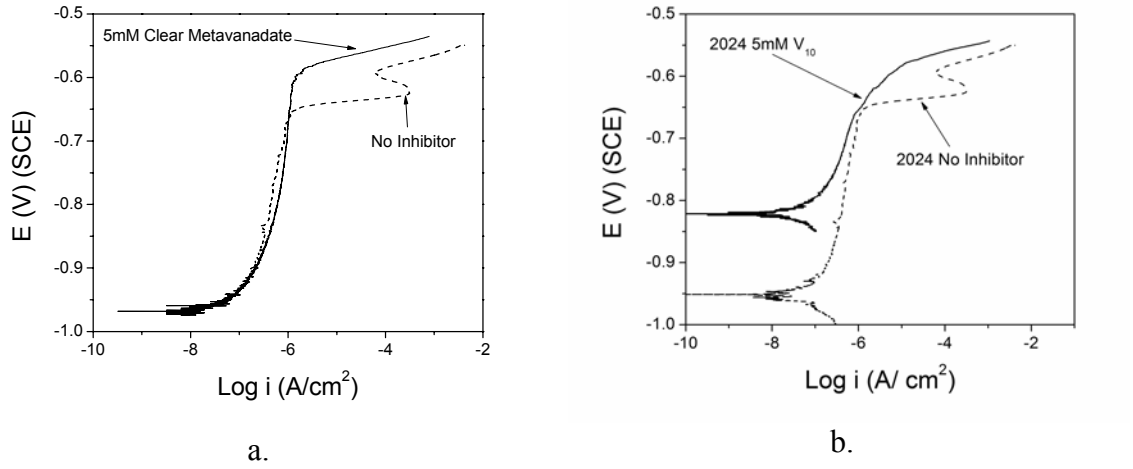

a. b.

Figure 5. Anodic polarization curves of AA2024-T3 in deaerated 0.5 M NaCl a) with and without 5 mM clear metavanadate, b) with and without 5 mM decavanadate (33).

Downloaded 29 Jun 2011 to 128.146.58.90. Redistribution subject to ECS license or copyright; see http://www.ecsdl.org/terms_use.jsp

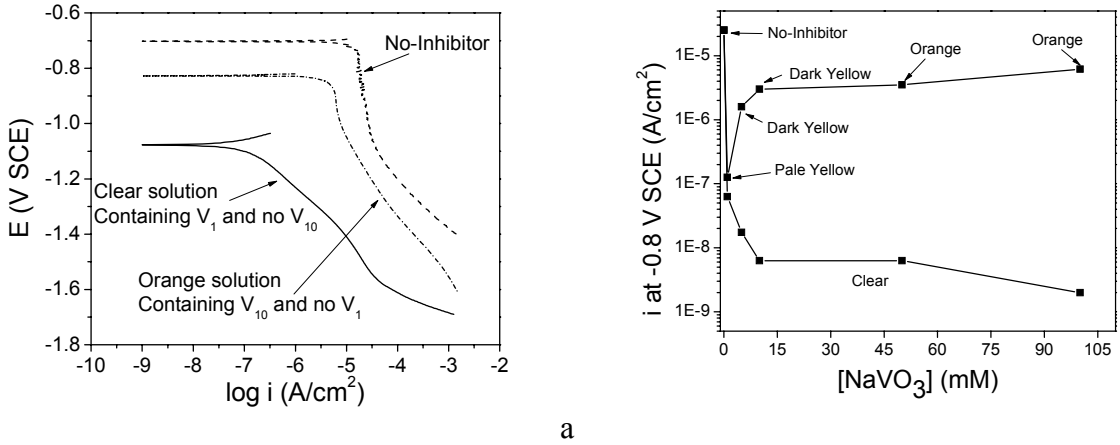

a b

Figure 6. Inhibition of ORR by vanadate solutions. a) Cathodic polarization curves of AA2024-T3 in 0.5M NaCl with no inhibitor, orange decavanadate, or clear metavanadate b) Effects of vanadate concentration on inhibition efficiency measured by calculating the cathodic current at E = -800mV SCE (20).

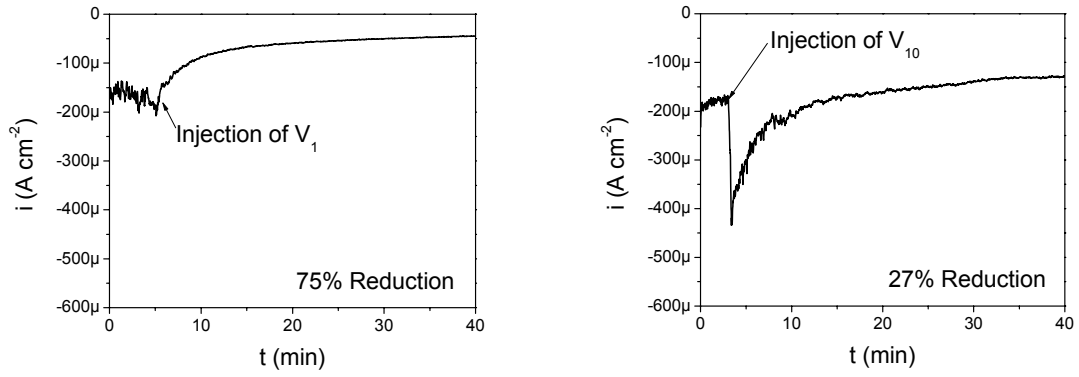

a b

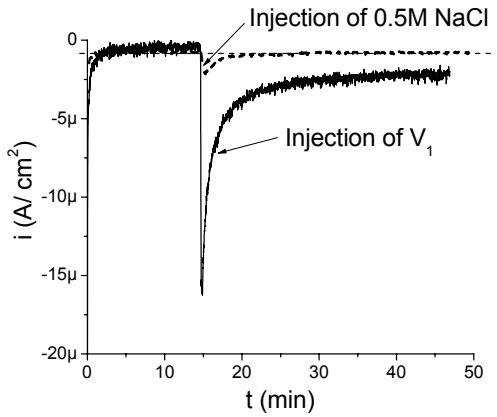

c

Figure 7. Chronoamperometry of Cu in aerated 0.5 M NaCl at -600 mV SCE. a) effects of clear metavanadate injections, b) effects of orange decavanadate injections, and c) effects of deaeration on injection of clear metavanadate (33).

Downloaded 29 Jun 2011 to 128.146.58.90. Redistribution subject to ECS license or copyright; see http://www.ecsdl.org/terms_use.jsp

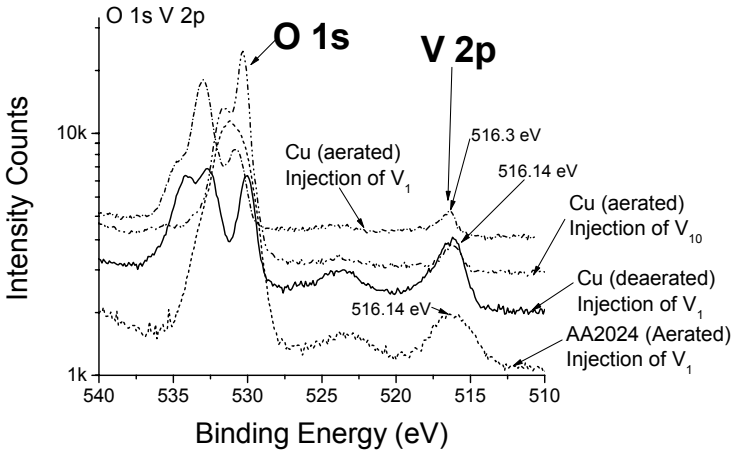

Figure 8. Oxygen 1s Vanadium 2p spectra after 2h exposure to solutions containing monovanadates or decavanadates at fixed potential under different aeration conditions as indicated. Cu sampled held at -600mV SCE and AA2024 samples held at -900 mV SCE (33).

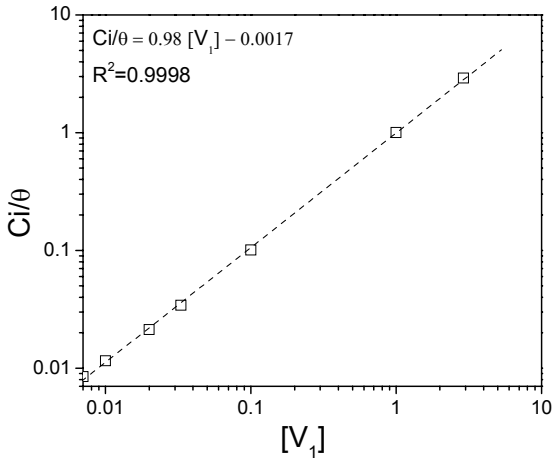

Figure 9. Adsorption isotherm adjusted by the Langmuir equation. (33)

Downloaded 29 Jun 2011 to 128.146.58.90. Redistribution subject to ECS license or copyright; see http://www.ecsdl.org/terms_use.jsp

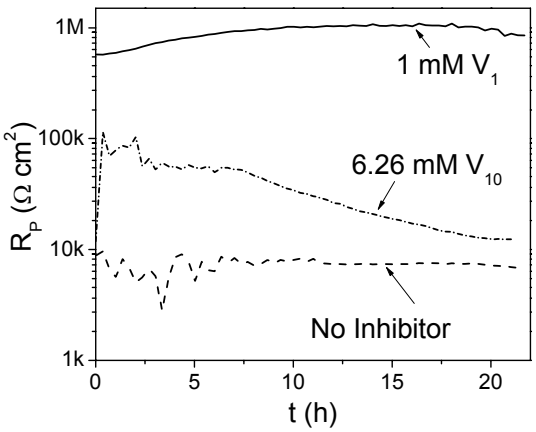

Figure 10. Polarization resistance of AA2024-T3 in 0.5M NaCl solutions containing no inhibitor, 1mM V_1 or 6.26 mM V_{10}. (20)

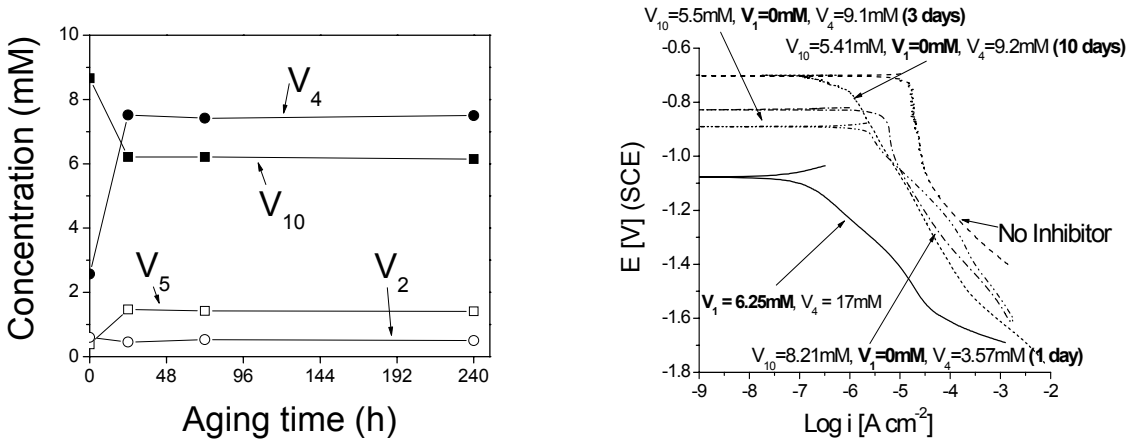

a b

Figure 11. Effects of solution aging on: a) speciation, and b) cathodic behavior of AA2024-T3 in orange decavanadate solutions. (20)

Downloaded 29 Jun 2011 to 128.146.58.90. Redistribution subject to ECS license or copyright; see http://www.ecsdl.org/terms_use.jsp

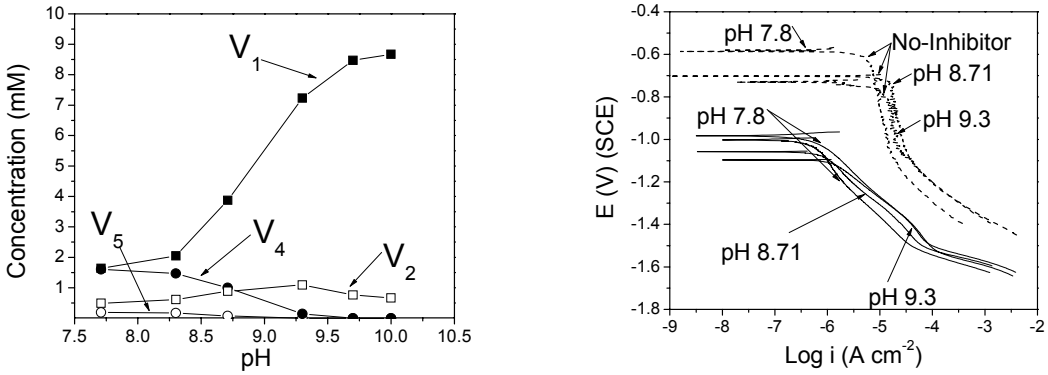

a b

Figure 12. a) Changes in speciation of clear metavanadate solutions as a function of pH, and b) Effects of pH and speciation on the kinetics of oxygen reduction on A2024-T3 (20).

Downloaded 29 Jun 2011 to 128.146.58.90. Redistribution subject to ECS license or copyright; see http://www.ecsdl.org/terms_use.jsp